7-1-2017

Accounting for photodegradation dramatically improves prediction of carbon losses in dryland systems

E. Carol Adair
University of Vermont

William J. Parton
Colorado State University

Jennifer Y. King
University of California, Santa Barbara

Leslie A. Brandt
USDA Forest Service

Yang Lin
University of California, Santa Barbara

Recommended Citation

ECOSPHERE

Accounting for photodegradation dramatically improves prediction of carbon losses in dryland systems

E. CAROL ADAIR,[1],† WILLIAM J. PARTON,[2] JENNIFER Y. KING,[3] LESLIE A. BRANDT,[4] AND YANG LIN[3]

[1]*Rubenstein School of Environment and Natural Resources, University of Vermont, Burlington, Vermont 05405 USA*
[2]*Natural Resource Ecology Laboratory, and Graduate Degree Program in Ecology, Colorado State University, Fort Collins, Colorado 80523 USA*
[3]*Department of Geography, University of California, Santa Barbara, California 93106 USA*
[4]*Northern Institute of Applied Climate Science, USDA Forest Service, Saint Paul, Minnesota 55108 USA*

Abstract. Traditional models of decomposition fail to capture litter mass loss patterns in dryland systems. This shortcoming has stimulated research into alternative drivers of decomposition, including photodegradation. Here, we use aboveground litter decomposition data for dryland (arid) sites from the Long-term Intersite Decomposition Experiment Team data set to test hypotheses (models) about the mechanisms and impacts of photodegradation. Incorporating photodegradation into a traditional biotic decomposition model substantially improved model predictions for mass loss at these dryland sites, especially after four years. The best model accounted for the effects of solar radiation via photodegradation loss from the intermediate cellulosic and lignin pools and direct inhibition of microbial decomposition. Despite the concurrent impacts of photodegradation and inhibition on mass loss, the best photodegradation model increased mass loss by an average of 12% per year compared to the biotic-only decomposition model. The best model also allowed soil infiltration into litterbags to reduce photodegradation and inhibition of microbial decomposition by shading litter from solar radiation. Our modeling results did not entirely support the popular hypothesis that initial lignin content increases the effects of photodegradation on litter mass loss; surprisingly, higher initial lignin content decreased the rate of cellulosic photodegradation. Importantly, our results suggest that mass loss rates due to photodegradation may be comparable to biotic decomposition rates: Mass loss due to photodegradation alone resulted in litter mass losses of 6–15% per year, while mass loss due to biotic decomposition ranged from 20% per year during early-stage decomposition to 3% per year during late-stage decomposition. Overall, failing to account for the impacts of solar radiation on litter mass loss under-predicted long-term litter mass loss by approximately 26%. Thus, not including photodegradation in dryland decomposition models likely results in large underestimations of carbon loss from dryland systems.

Key words: cellulose; lignin; litter decomposition; Long-term Intersite Decomposition Team (LIDET); photodecomposition; UV.

† **E-mail:** Carol.Adair@uvm.edu

INTRODUCTION

Traditional decomposition models fail to accurately predict aboveground decomposition in arid systems, underestimating mass loss and overestimating nitrogen immobilization (Parton et al. 2007, Adair et al. 2008). This failure has stimulated research into novel drivers of decomposition. Chief among these is photodegradation, the breakdown of organic matter by shortwave

visible and ultraviolet solar radiation (280–550 nm; Brandt et al. 2009, Austin and Ballaré 2010, Austin et al. 2016).

Research indicates that exposure to shortwave radiation increases carbon (C) mineralization from litter and soil organic matter, but the mechanistic details of this process remain uncertain. For example, debate continues regarding the specific C compound(s) photodegraded in plant litter (King et al. 2012). While it has been assumed that litter lignin is the compound most susceptible to photodegradation (and therefore mineralized), there is conflicting evidence supporting this assumption (Rozema et al. 1997, Brandt et al. 2007, 2010, Day et al. 2007), and in some cases, mass loss has been observed from litter hemicellulose rather than lignin (Brandt et al. 2010, Baker and Allison 2015, Lin et al. 2015a). Austin and Ballaré (2010) found that photodegradation did not occur in a pure cellulose (i.e., lignin-free) substrate, but only occurred when lignin was present and increased with lignin concentration. Although these patterns were consistent with photodegradation of lignin (Austin and Ballaré 2010), it has also been suggested that lignin induces the breakdown of other compounds via indirect photolysis: The UV (280–400 nm) radiation absorbed by photoreactive lignin may produce free radicals that break bonds in other compounds, such as hemicellulose, in the lignocellulose matrix (Schade et al. 1999, Brandt et al. 2010, Baker and Allison 2015).

Furthermore, shortwave radiation may have complex effects on biotic litter decomposition. Exposure to shortwave radiation (UV-A and UV-B) may slow biotic decomposition via negative impacts on microbes (Mitchell and Karentz 1993, Johanson et al. 1995, Kielbassa et al. 1997, Caldwell et al. 1998, Johnson 2003, Kurbanyan et al. 2003, Fernández Zenoff et al. 2006, Lin et al. 2015b), but enhance biotic decomposition via the production of labile photodegraded material (e.g., Gallo et al. 2006, Foereid et al. 2011, Baker and Allison 2015, Wang et al. 2015).

Another process that may drive dryland decomposition is soil–litter mixing, which may have both positive and negative impacts on mass loss. Soil–litter mixing may shade litter from sunlight, thereby reducing photodegradation, but may also shield decomposers from UV radiation, enhancing biotic decomposition (Barnes et al. 2012). Mixing may also enhance decomposition by promoting microbial litter colonization, physically abrading litter, and buffering litter from extreme heat and aridity (Throop and Archer 2009, Hewins et al. 2013, Lee et al. 2014). Although soil–litter mixing could explain some of the increased mass loss, it fails to account for the observed lack of litter N immobilization in dryland systems (Parton et al. 2007).

To tease apart the relative roles of abiotic and biotic decomposition processes and their underlying mechanisms, we used data from the arid (or dryland) sites in the Long-term Intersite Decomposition Team (LIDET) data set (LIDET 1995) to test hypotheses regarding the role of photodegradation and soil–litter mixing in dryland decomposition. To the best of our knowledge, the LIDET data set contains the only long-term data for aboveground litter decomposition in arid systems. Here, litter mass loss followed an atypical linear mass loss pattern suggestive of photodegradation, which becomes particularly apparent after four to six years of mass loss (Fig. 1). We used these data to test a suite of models that examined the overall hypothesis that litter mass loss at these sites is governed by both biotic decomposition and photodegradation and that the balance between these two processes would be impacted by soil–litter mixing. Specifically, we hypothesized that (1) litter mass loss associated with photodegradation will be from the cellulosic pool, but may be enhanced in litter with high lignin content via indirect photolysis; (2) photodegradation breaks down complex C into simple C that is added to labile C pools, thereby enhancing biotic decomposition; (3) exposure to solar radiation decreases decomposition of labile carbon via negative impacts on soil decomposer populations; and (4) soil infiltration (characterized by ash content) reduces the exposure of litter to solar radiation, thereby decreasing photodegradation and negative impacts on soil decomposers.

We developed mechanistic models to test these hypotheses and compared them using likelihood methods.

Methods

LIDET dryland data

Long-term Intersite Decomposition Team was initiated in 1990 to study the impacts of climate
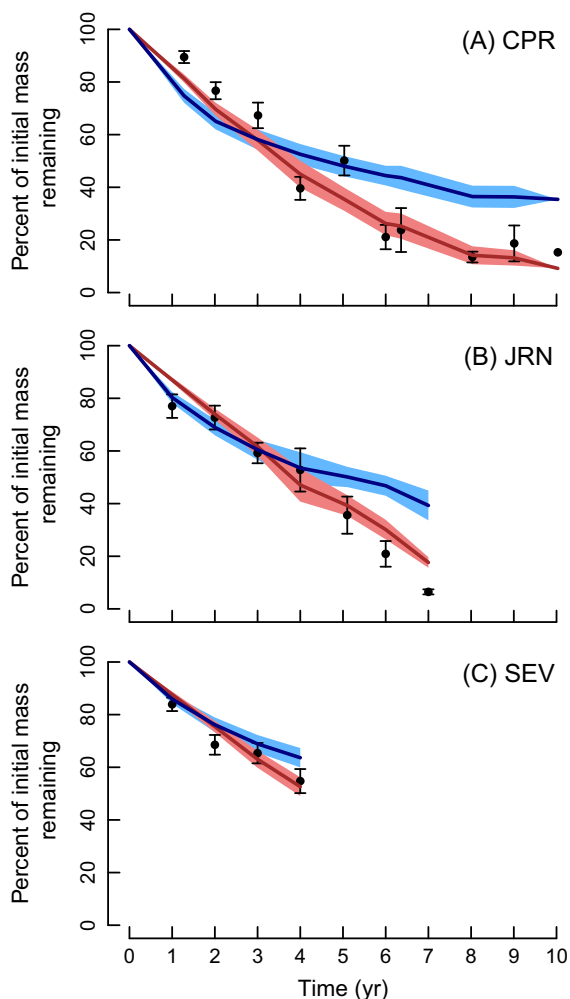
Fig. 1. Percent mass remaining over time at (a) Central Plains Experimental Range (CPR), (b) Jornada Experimental Range (JRN), and (c) Sevilleta National Wildlife Refuge (SEV), averaged across litter types. Black dots are observations ±1 SE. Predictions from the best photodegradation (red lines) and biotic-only (blue lines) models are shown. Shaded areas are ±1 SE for model predictions. Note: At time 10, there are not enough data/predictions to calculate SE.

(Table 1). The sites differ somewhat in mean annual temperature and precipitation, with SEV and JRN being somewhat hotter and drier than CPR (Table 1). Sevilleta receives 60% of its precipitation as summer monsoon rains (June–September), with the rest as winter storm fronts (Brandt et al. 2010). Similarly, JRN receives approximately 60% of its total precipitation during intense, spatially heterogeneous late summer monsoons (July–September; Hewins et al. 2013). In contrast, the precipitation pattern at CPR is not driven by monsoons, but the site receives relatively low precipitation from November to March and higher precipitation during the growing season (April–October).

Eight types of leaf litter were decomposed at these sites, including the six standard litter types included at all LIDET sites (Table 2). Leaf litter (10 g) was incubated in 20×20 cm litterbags with a top nylon mesh of 1 or 7 mm and a bottom mesh of 55-μm DACRON cloth. While termite-induced mass loss was not specifically noted in the 1-mm-mesh bags at the three arid sites, a comparison of small (1 mm) and large (7 mm) mesh bags during the first two years did indicate that termites were important at JRN when they could get into the bags (M. E. Harmon, *personal communication*). We therefore excluded the 7-mm-mesh bags from this analysis. At each site, four locations (replicates) were selected to represent the range of typical

and substrate quality on leaf and root litter decomposition over 10 yr (LIDET 1995, Gholz et al. 2000). We investigated patterns of aboveground leaf decomposition from the project's three arid, or dryland, sites: Central Plains Experimental Range in Colorado (CPR) and Jornada Experimental Range (JRN) and Sevilleta National Wildlife Refuge (SEV) in New Mexico

Table 1. Climatic characteristics of the three LIDET dryland sites: Central Plains Experimental Range (CPR), Jornada Experimental Range (JRN), and Sevilleta National Wildlife Refuge (SEV).

SITE	CPR	JRN	SEV
LAT (degrees)	40.82	32.50	34.33
LONG (degrees)	104.77	106.75	106.67
ELEV (m)	1650	1410	1572
MAP (mm)	440	298	255
MAT (°C)	8.60	17.15	13.17
AET (mm)	430	292	252
PET (mm)	1202	1666	1602
CDI_{LT}	0.243	0.216	0.136
Total years	10	7	4

Notes: All climatic variables were calculated for the 10 yr of available data closest to the LIDET study period (1990–1999). CDI_{LT} is the Lloyd and Taylor (1994) climatic decomposition index (CDI). Total years = the number of years leaf litter was decomposed at each site.

Table 2. Initial values of litter quality indices for species in the Long-term Intersite Decomposition Team study.

Species	Litter type	Abbreviations	Cellulose (%)	Lignin (%)	C (%)	N (%)	C/N	$L_s = L/(L + \text{Cell})$
Sugar maple† (*Acer saccharum*)	Broadleaf	ACSA	27.33	15.87	49.77	0.81	61.83	0.367
Drypetes† (*Drypetes glauca*)	Broadleaf	DRGL	39.82	10.91	47.79	1.97	24.25	0.215
Tulip poplar (*Liriodendron tulipifera*)	Broadleaf	LITU	31.27	8.70	46.36	0.72	65.06	0.218
Red pine† (*Pinus resinosa*)	Conifer	PIRE	44.58	19.18	53.41	0.59	92.72	0.301
Chestnut oak† (*Quercus prinus*)	Broadleaf	QUPR	39.38	23.51	51.48	1.03	50.55	0.374
Pacific rhododendron (*Rhododendron macrophyllum*)	Broadleaf	RHMA	36.90	16.95	50.80	0.42	126.28	0.315
Western redcedar† (*Thuja plicata*)	Conifer	THPL	35.92	26.67	51.13	0.62	83.12	0.426
Wheat† (*Triticum aestivum*)	Grass	TRAE	73.15	16.21	47.32	0.38	133.32	0.181

Notes: L, lignin; N, nitrogen; C, carbon. Each dryland site had six standard aboveground litter types.
　† One of the six "standard" species decomposed at each site.

conditions. Litterbags were placed flat on top of the existing litter layer and were collected annually at CPR, JRN, and SEV for 10, 7, and 4 yr, respectively (see Appendix S1 for site photographs of bag placements at SEV and JRN). Bags were installed at CPR in November 1990, at JRN in November and December 1990, and at SEV in October 1990. Bags were collected each year in October, November, February (one time in 1992), or March (one time in 1997) at CPR, in November or December at JRN (prior to or at the beginning of the winter precipitation period), and in October or November at SEV (for more details, see LIDET 1995, Harmon et al. 2009).

We also note that traditional mesh bags, such as the ones used here, effectively shade litter from exposure to UV radiation (Brandt et al. 2010). Thus, our results may be an underestimation of mass loss due to photodegradation. However, the 1-mm nylon mesh used in the LIDET study is reported to block only 10% of incoming UV-B radiation (280–320 nm), compared to fiberglass mesh that blocks 45–50% (Pancotto et al. 2005, Brandt et al. 2007, Uselman et al. 2011). Additionally, our literature survey of field UV radiation studies, expanded from the set included in King et al. (2012), found no significant mean differences ($P > 0.1$) in mass loss rates among mesh/container types, although mass loss rates from litter in clear plastic containers tended to be higher (mesh mass loss rates averaged 1.1–1.8 g/month vs. 2.8 g/month for plastic containers; Appendix S2).

Initial litter *C*-to-*N* ratios (*C/N*) ranged from 24 to 126, initial lignin contents ranged between 9% and 27%, and initial cellulose values were 27–73%

(Table 2). Initial litter *C* and *N* contents were determined using a Leco C/N/S-2000 Macro Analyzer (Leco, St Joseph, Michigan, USA). Initial litter acid-non-hydrolyzable fraction, traditionally considered lignin, was determined by hydrolyzing extractive-free material with sulfuric acid and weighing the residue (Effland 1977, Obst and Kirk 1988). The acid-hydrolyzable fraction was considered to be cellulose (McClaugherty et al. 1985, Ryan et al. 1990). Initial litter ash content was determined by heating a sample of litter in a muffle furnace at 450°C for 8 h. The mass of the remaining material was divided by the initial mass to determine the fraction of litterbag contents that was ash (Harmon et al. 2009). For decomposed litter, ash and *N* contents were determined as above on a subsample of collected litter. All decomposed litter samples were analyzed using a NIRS 6500 infrared spectrophotometer (FOSS, Silver Springs, Maryland, USA). Ash and *N* contents were correlated with the near infrared reflectance (NIR) spectra. This correlation was used to predict ash and *N* contents for the remaining samples. For more details on the LIDET experimental design and methods, see LIDET (1995).

Biotic decomposition model

Models were based on a biotic decomposition model that was previously developed using the entire LIDET data set (27 sites, 29 leaf and root litter types; Adair et al. 2008). This three-pool exponential model served as a null hypothesis of biotic decomposition only (the biotic-only model), with a fast pool representing labile carbon decomposition, an intermediate pool representing cellulose (including cellulose encrusted

or protected by lignin) decomposition, and a slow pool representing lignin decomposition. The initial size of the slow pool (M_3) is equal to initial lignin (L) content of each litter. Initial sizes of the labile and intermediate pools are determined by the initial litter lignin-to-nitrogen ratio (L/N) such that the size of the labile pool (M_1) decreases (and the size of the intermediate pool, M_2, increases) exponentially with increasing L/N to a minimum labile pool size at $L/N = 60$:

$$M_1 = \begin{cases} b_1 e^{(-b_2 \frac{L}{N})} & \text{if } \frac{L}{N} \leq 60 \\ b_1 e^{(-b_2 60)} & \text{if } \frac{L}{N} > 60 \end{cases} \quad (1)$$

where b_1 and b_2 are fitted parameters. Each pool loses mass exponentially at a decomposition rate, which is modified by litter quality and climate:

$$\begin{aligned} M(t) = {} & M_1(0)e^{-k_1 \text{CDI}_{\text{LT}} t} \\ & + M_2(0)e^{-k_2 \text{CDI}_{\text{LT}} e^{(-bL_s)} t} \quad (2) \\ & + M_3(0)e^{-k_3 \text{CDI}_{\text{LT}} t} \end{aligned}$$

where $M(t)$ is the percent of initial litter mass remaining at time, t; $M_i(0)$ is the initial size of the labile ($i = 1$), intermediate ($i = 2$), or slow ($i = 3$) pool; k_i is the decomposition rate of each pool; and CDI_{LT} is a climatic decomposition index (CDI) that is a multiplicative function of a water stress function (based on monthly precipitation and potential evapotranspiration) and the Lloyd and Taylor (LT; 1994) variable Q_{10} temperature function (Adair et al. 2008). The decomposition rate of the intermediate pool (k_2) is modified by the initial litter lignin fraction such that k_2 decreases with increasing lignin fraction, L_s: $e^{(-b \times L_s)}$, where b is a fitted parameter and $L_s = L/(L + \text{cellulose})$. This accounts for protection or "encrustation" of cellulose by lignin, which ultimately limits the decomposition of cellulose in the lignin–carbohydrate matrix of plant cell walls (Berg et al. 1982, 1984, McClaugherty and Berg 1987, Aber et al. 1990, Chesson 1997). This "biotic-only" model and model development are described in detail in Adair et al. (2008).

We modified the biotic-only model to test hypotheses regarding the effects of shortwave radiation on decomposition. To maintain consistency with our previous investigation of biotic decomposition, the biotic-only model was not re-parameterized for this model comparison. We used parameters derived from the entire LIDET data set ($k_1 = 3.5454$, $k_2 = 0.7471$, $k_3 = 0.0270$, $b = 1.3243$, $b_1 = 57.1669$, $b_2 = 0.0301$; Adair et al. 2008).

Hypothesis 1: photodegradation of cellulose vs. lignin

In a laboratory setting, Brandt et al. (2009) found that, unlike biotic decomposition, production of CO_2 from photodegradation was dependent not on litter mass, but on surface area and that CO_2 was produced at a constant (linear) rate. Based on these results, we added photodegradation fluxes to the biotic-only model as constant or zero-order flows from cellulosic and/or lignin pools (i.e., rates are not dependent on the size of the pool):

$$\frac{dM_2}{dt} = -k_2 M_2(t)\text{CDI}_{\text{LT}} e^{-bL_s} - p_2 S_{\text{in}} \quad (3)$$

$$\frac{dM_3}{dt} = -k_3 M_3(t)\text{CDI}_{\text{LT}} - p_3 S_{\text{in}}, \quad (4)$$

where $M_i(t)$ is the size of the intermediate pool ($i = 2$) or slow pool ($i = 3$), at time, t; k_i is the biotic decomposition rate for pool 2 or 3; $p_i S_{\text{in}}$ is mass loss from pool 2 or 3 due to photodegradation (p); and S_{in} is mean annual solar radiation in W/m^2 (1990–1999; North American Regional Reanalysis [NCEP] 2004). Note that if M_i minus the photodegradation flux was <0, then M_i was set equal to zero (i.e., pool sizes were not allowed to be negative). We used annual solar insolation instead of specific radiation wavelength bands in order to make the model as accessible and generalizable as possible. Availability of wavelength-specific data is limited, as are data on the action spectra of photodegradation vs. microbial inhibition.

To test our first hypothesis, we tested model versions with photodegradation fluxes from only the intermediate pool (M_2), only the slow pool (M_3), or both pools. To test the hypothesis that initial litter lignin content or lignin fraction enhances photodegradation of the cellulosic or intermediate pool (e.g., by producing free radicals), we created models that allowed mass loss from the intermediate pool to increase/decrease with the initial lignin fraction (L_s) or lignin

content (Table 2). This relationship is not well understood, but Austin and Ballaré (2010) found that mass loss increased linearly with increasing lignin concentration. Thus, we constrained our model development to investigate only a linear relationship, allowing increasing amounts of lignin or lignin fractions to increase photodegradation from a theoretical minimum at a lignin content or lignin fraction of zero (note, however, that we did not constrain l_1 to positive values, as Chen et al. (2016) found that photodegradation decreased with increasing initial lignin content):

$$\frac{dM_2}{dt} = -k_2 M_2(t)\mathrm{CDI}_{\mathrm{LT}}e^{-bL_s} \\ - p_2 S_{\mathrm{in}}(1 + l_1\mathrm{Lig}) \qquad (5)$$

$$\frac{dM_3}{dt} = -k_3 M_3(t)\mathrm{CDI}_{\mathrm{LT}} - p_3 S_{\mathrm{in}}(1 + l_1\mathrm{Lig}), \quad (6)$$

where Lig is either initial lignin fraction, L_s, or initial lignin content as a fraction of initial mass ($M_3/100$) and l_1 is a fitted parameter. We also tested model versions that fit an intercept term (i.e., $l_2 + l_1\mathrm{Lig}$), but attempts to fit this model often failed or never produced a better model than the above version with the intercept set equal to one.

Hypothesis 2: facilitation of decomposition via photodegradation products

We created models that allowed a fraction of the photodegradation flux (p_i) from the intermediate and/or slow pools to enter the labile pool (M_1) as labile carbon:

$$\frac{dM_1}{dt} = -k_1 M_1(t)\mathrm{CDI}_{\mathrm{LT}} + f(p_i S_{\mathrm{in}}), \qquad (7)$$

where $p_i S_{\mathrm{in}}$ is the photodegradation flux from M_2 or M_3, and f is the fraction of $p_i S_{\mathrm{in}}$ added to the fast or labile pool, M_1. If both pools contained a photodegradation flux, for model simplicity (to maintain a reasonable number of estimated parameters), the same fraction of each flux was added to M_1:

$$\frac{dM_1}{dt} = -k_1 M_1(t)\mathrm{CDI}_{\mathrm{LT}} + f(p_2 S_{\mathrm{in}}) + f(p_3 S_{\mathrm{in}}) \quad (8)$$

Photodegradation flows to M_1 from only the intermediate pool, only the slow pool, or from both pools were added to the appropriate model(s) from Hypothesis 1 (Table 3).

Hypothesis 3: inhibition of biotic decomposition by exposure to shortwave radiation

Each of the models from Hypotheses 1 and 2 was compared against a version that reduced the microbial decomposition rates of all pools (k_1, k_2, and k_3) as a linear function of S_{in}. For example:

$$\frac{dM_1}{dt} = (1 - rS_{\mathrm{in}})(-k_1 M_1(t)\mathrm{CDI}_{\mathrm{LT}} \\ + f(p_2 S_{\mathrm{in}}) + f(p_3 S_{\mathrm{in}}) \qquad (9)$$

$$\frac{dM_2}{dt} = (1 - rS_{\mathrm{in}})(-k_2 M_2(t)\mathrm{CDI}_{\mathrm{LT}}e^{-bL_s}) \\ - p_2 S_{in} \qquad (10)$$

$$\frac{dM_3}{dt} = (1 - rS_{\mathrm{in}})(-k_3 M_3(t)\mathrm{CDI}_{\mathrm{LT}}) - p_3 S_{\mathrm{in}}, \quad (11)$$

Table 3. Best models selected by AICc from the model set (59 models) with the biotic-only null model (Model 1) for comparison.

Model	p_2 (SE)	p_3 (SE)	f (SE)	r (SE)	l_2 (SE)	a (SE)	K	dAICc	R^2	Model rank
1	. . .	. . .	. . .	. . .	. . .	. . .	1	103.8	0.7249	55
42	0.033 (0.002)	0.003 (0.0013)	. . .	0.002 (0.0001)	−2.38 (0.154)	0.301 (0.202)	6	0	0.8502	1
54	0.029 (0.001)	. . .	. . .	0.002 (0.0001)	−1.954 (0.144)	0.251 (0.048)	5	7.5	0.8419	2
34	0.008 (0.001)	0.005 (0.0003)	. . .	0.001 (0.0001)	. . .	0.001 (0.002)	5	925.3	0.8216	14
41	0.008 (0.000)	0.005 (0.0002)	0.371 (0.096)	0.001 (0)	−0.018 (0.017)	0.005 (0.000)	7	931.2	0.8195	17
13	0.003 (0.001)	0.005 (0.0003)	. . .	0.001 (0.0001)	4.189 (0)	. . .	5	934.2	0.8114	19
39	0.001 (0.001)	0.004 (0.0003)	. . .	. . .	0.003 (0)	0.01 (0.008)	5	958.8	0.7896	46

Note: The best model had a dAICc = 0 (Model 42). p_i = the rate of photodegradation from pool i (either M_2 or M_3); f = fraction of flow from photodegradation that is returned to M_1 (the fast pool; $1 - f$ = the amount mineralized); r = constant for reduction in the fast decomposition rate (k_1); a = constant for reduction in photodegradation due to shading from infiltrated sediment; SE = standard error as calculated by mle2.

where r is the biotic decomposition reduction parameter, which has a value between 0 and 1 that fractionally reduces k_1, k_2, and k_3 as a function of mean annual solar radiation, S_{in} (if $r = 0$, there is no reduction in biotic decomposition; Table 3).

Hypothesis 4: reduction in photodegradation effects by soil infiltration

In litterbag studies, soil–litter mixing manifests as soil infiltration, which can be examined, at least in part, using the ash content of collected litterbags (e.g., Throop and Archer 2007). Ash content includes both litter ash and mineral soil infiltration. Assuming that litter ash remains relatively constant over time, we use variation in ash content to examine how litter decomposition changes with varying degrees of soil infiltration.

It has been suggested that soil–litter mixing has a uniquely positive effect on decomposition in dryland systems (e.g., Throop and Archer 2007, Lee et al. 2014). However, in the LIDET data set, we found evidence of a positive effect of soil–litter mixing on mass loss in both arid and mesic grasslands and the impact of soil–litter mixing on mass loss appeared to be greater in mesic than in arid grasslands (Appendix S3: Figs. S1, S2). Across arid grassland sites and litter types, litter mass remaining declined with increasing ash content at three of ten time points: years 2, 4, and 6. At these time points, variation in ash content explained approximately 20, 30, and 40% of the variation in mass remaining, respectively (Appendix S3: Fig. S1). In humid grasslands, negative relationships between percent ash and mass remaining had stronger relationships in more years: years 2, 3, 7, 8, and 10. At these time points, variation in ash content explained 30–80% of the variation in mass remaining (Appendix S3: Fig. S2). These results suggest that the positive impact of soil infiltration on mass loss may not be a mechanism unique to arid lands and is likely already accounted for in our biotic-only null model (although not explicitly). Thus, we confined our investigation of soil–litter mixing impacts to shading effects by allowing percent ash to reduce the exposure of litter to solar radiation. We created models that allowed soil–litter mixing to reduce mass loss via photodegradation (p_i) and reduce the inhibition of decomposers (r) via UV and shortwave radiation exposure as in the following example equations for a model where photodegradation losses are only from the intermediate pool:

$$\frac{dM_1}{dt} = (1 - r(S_{in}e^{-a\text{ASH}}))(-k_1M_1(t)\text{CDI}_{LT}) + f(p_2(S_{in}e^{-a\text{ASH}})) \quad (12)$$

$$\frac{dM_2}{dt} = (1 - r(S_{in}e^{-a\text{ASH}}))(-k_2M_2(t)\text{CDI}_{LT}e^{-bL_S}) - p_2(S_{in}e^{-a\text{ASH}}) \quad (13)$$

$$\frac{dM_3}{dt} = (1 - r(S_{in}e^{-a\text{ASH}}))(-k_3M_3(t)\text{CDI}_{LT}), \quad (14)$$

where ASH is the fraction of the litter sample that is ash and a is a fitted parameter that determines the rate of decrease for p_2, p_3, or r toward zero. We also investigated a model that linearly decreased photodegradation (by reducing exposed litter surface area; e.g., p_2 $(1 - a\text{ASH})$), but parameterization of this equation nearly always yielded unrealistic mass addition processes (e.g., negative values of p_2, which added mass to M_2). We therefore used the above exponential equation, which can only reduce the terms p_2, p_3, or r toward zero. This resulted in a total of 59 models, including the biotic-only null model, which we compared using the LIDET dryland data (model list and results in Appendix S4).

Statistical analysis

To test the above hypotheses, we used the set of 59 above-described models, which were developed based on our well-tested biotic-only null model (Adair et al. 2008) and our current understanding of photodegradation mechanisms. Each of these models was fit and parameterized using the LIDET dryland data set. We then used Akaike's Information Criterion modified for small sample sizes (AICc) to choose among these models. The model with the lowest AICc value has the most support in the data (Burnham and Anderson 2002). Differences between the AICc value of the best model and the values of models ranked below it (dAICc = AICc of each model—AICc best model) provide information to evaluate whether models in the set are close competitors to the best model: The dAICc of the best model is zero; models with a dAICc ≤ 3 have substantial support in the data; models with dAICc > 7 have

essentially no support in the data relative to the best models (Burnham and Anderson 2002). This methodology also provides information on model selection uncertainty via Akaike weights, which are the probability that the model would be selected as best, given the same models and a new similar but independent data set (Burnham and Anderson 2002). In evaluating model selection results, we also took into account the ecological and practical significance of each parameter: whether the effect size was large (ecologically relevant) or near zero and whether the parameter estimate could be considered different from zero based on its standard error (SE; i.e., whether the t statistic—parameter estimate/parameter SE—for the parameter was greater than 2 and whether the parameter estimate ±1 SE included zero). All statistical analyses were performed in R 3.3.2 (R Core Team 2016). All models were fit using mle in the bbmle package (Bolker and the R Development Core Team 2016).

RESULTS

The best model dramatically improved prediction of mass loss in arid systems and all other models had a dAICc > 7, indicating very strong support for this model compared to all other models in the model set (Fig. 1, Table 3; Appendix S4). Only one other model had a dAICc < 10 (dAICc = 7.5; Table 3; Appendix S4). All other models had dAICc values > 10, indicating essentially no support in the data relative to the best model (Appendix S4).

The best model (1) had photodegradation losses from the intermediate cellulosic and lignin pools, (2) did not enhance biotic decomposition indirectly by breaking down cellulosic or lignin C into labile C, (3) inhibited microbial decomposition by reducing biotic decomposition rates, and (4) allowed soil infiltration (characterized by ash content) to reduce UV radiation impacts on mass loss and inhibition of biotic decomposition (Table 3). The second best model contained these same characteristics, but did not include photodegradation from the lignin pool (dAICc = 7.5, but note that a dAICc > 7 indicates essentially no support in the data relative to the best model(s); Table 3).

The best model better predicted mass loss (R^2 = 85%) than the biotic-only decomposition model (R^2 = 72%; Table 3) and captured the patterns of mass loss observed across all three sites, particularly after years 4 and 5 (Fig. 1). For short decomposition periods (i.e., <4 yr), the biotic-only and best photodegradation models both captured the general pattern of aboveground litter decomposition, but observed data and the best photodegradation model predictions increasingly diverged from biotic-only model predictions as the decomposition period lengthened (Fig. 1).

Across all 10 yr, the best photodegradation model increased mass loss by 12% per year compared to the biotic-only model (averaged across sites and litter types). Initially, the biotic model lost mass more quickly than the photodegradation model (3–5% more in years 1–2), but this trend reversed in year 3 with the net effect of exposure to solar radiation being to increase mass loss from 2% in year 3 to 26% in year 10 (in comparison with the biotic model; averaged across sites and litter types).

Hypothesis 1: photodegradation of cellulose vs. lignin

The best model enhanced litter mass loss by including a photodegradation flux from both the intermediate cellulosic and slow lignin pools. However, in contrast to our expectations of a positive impact of lignin on photodegradation, the best model also included a term that *decreased* photodegradation of the intermediate cellulosic pool as initial lignin content *increased* (Table 3).

In the best model, photodegradation alone increased mass loss from the intermediate cellulosic pool at a maximum rate of 13.6% per year at JRN, 13.4% per year at SEV, and 11.9% per year at CPR (averaged across litter types). However, because the rate varied not only as a function of average annual solar radiation, but also with ash content and initial lignin content, minimum rates were 4.9% per year at JRN, 4.8% per year at SEV, and 4.3% per year at CPR (due to high ash and initial lignin contents). Depending on ash content, photodegradation of the lignin pool ranged from 1.2% to 1.5% per year at JRN and SEV and 1.1% to 1.4% at CPR (averaged across litter types; photodegradation decreased with ash content).

In comparison, biotic mass loss from the cellulosic pool ranged between 0.4% and 1.3% per year during early-stage decomposition (defined as near 100% of initial cellulose remaining) at low to high ash contents, respectively, and

0.08–0.3% per year during late-stage decomposition (defined as 20% of initial cellulose remaining) at low to high ash contents (averaged across species and sites). Averaged across sites and species, annual lignin mass loss due to biotic decomposition ranged from 0.005% to 0.01% per year during early-stage decomposition and from 0.002% to 0.006% per year during late-stage decomposition, again increasing with ash content.

On average, across sites and litter types, total mass loss due to biotic decomposition (i.e., in the biotic-only model) ranged from 20% per year during early-stage decomposition to 3% per year during late-stage decomposition. In contrast, the best photodegradation model predicted slightly slower early-stage decomposition at 15% per year, but faster late-stage decomposition at 6.5% per year (declines were due to increasing ash content). Overall, our results indicate that photodegradation is an important mechanism for aboveground litter mass loss, comparable in size to biotically driven mass loss rates.

In the best photodegradation model, we also found that litter C fractions declined with strikingly different mass loss patterns compared to the biotic-only model (Fig. 2). At all time points, mass loss from the intermediate cellulosic and lignin pools was faster in the photodegradation

model than in biotic-only model, although more conspicuously so for the intermediate pool (Fig. 2). These faster mass loss rates resulted in the best photodegradation model predicting, on average, nearly 20% less cellulose remaining and 10% less lignin remaining by the end of the 10-yr decomposition period than were predicted by the biotic-only model.

Across litter types, mass loss *declined* with increasing lignin content over the entire sampling period, and mass remaining at 10 yr was largely dependent on the initial lignin content of each litter type (i.e., the majority of mass remaining at year 10 was in the lignin pool; Figs. 2, 3). We further examined the relationship between mass loss and initial lignin content by regressing percent of initial mass remaining at each time point vs. initial lignin content (Appendix S3: Fig. S3). At all but three time points, mass remaining increased with initial lignin content ($P < 0.1$ at time = 4 yr; $P < 0.05$ at time = 1, 2, 3, 5, 6, and 8 yr; Appendix S3: Fig. S3). Non-significant relationships at remaining time points may be related to an insufficient number of data points. There were no significant relationships between mass remaining and cellulose content at any time point.

The negative relationship between initial lignin content and rates of mass loss was formalized in
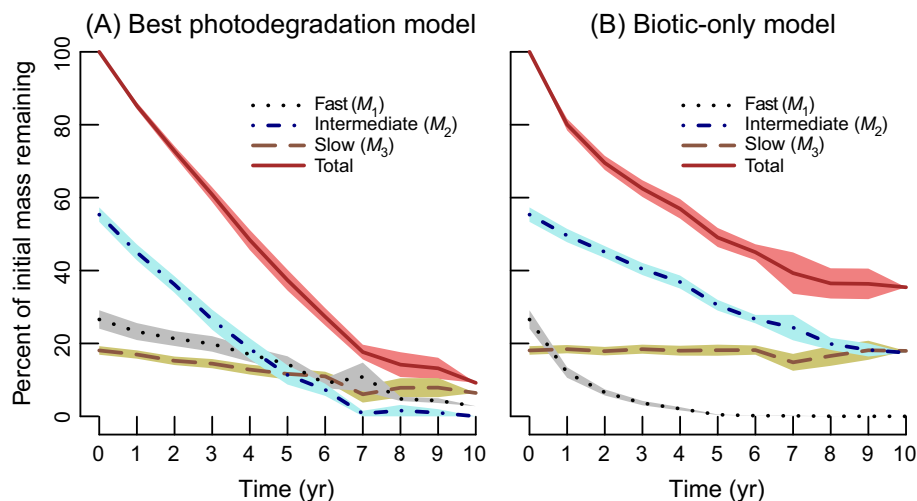

Fig. 2. Predicted percent mass remaining over time for total litter and each pool averaged across dryland sites (Central Plains Experimental Range, Jornada Experimental Range, and Sevilleta National Wildlife Refuge) and litter type for (a) the best photodegradation model and (b) the biotic-only model. Shaded areas are ±1 SE of averaged model predictions. Lines without error shading after time = 0 are a single prediction (i.e., $t = 10$).
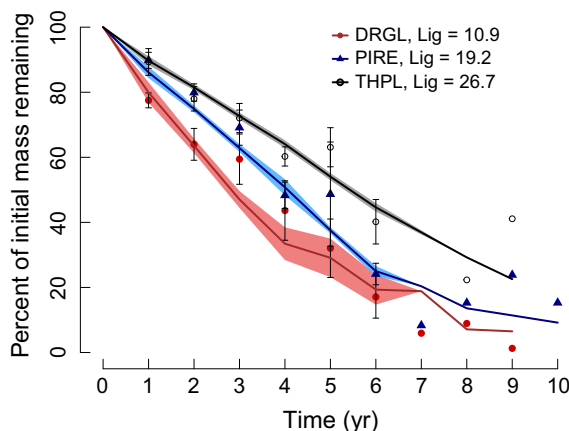
Fig. 3. Percent mass remaining over time averaged across sites for three litter types of differing initial lignin content: *Drypetes glauca* (DRGL), *Pinus resinosa* (PIRE), and *Thuja plicata* (THPL; Table 2). Lines are model predictions. Shaded areas are ±1 SE of averaged model predictions. Points are observed data ±1 SE. Points or lines without error bars or shading are a single measurement or prediction, respectively.

the best model by a term that reduced photodecomposition of the intermediate cellulosic pool based on initial lignin content. Our results, which were in contrast to our hypothesis that initial lignin content would *increase* the photodegradation of this pool, indicated that initial lignin decreased photodegradation by 5–7.3% (depending on site and litterbag ash content).

Hypothesis 2: facilitation of decomposition via photodegradation products

In contrast to our hypothesis, the best model did not enhance biotic decomposition by breaking down intermediate (cellulose) or lignin C and adding it to the fast pool as labile C. In fact, the models that included this term (f) all had a dAICc > 13, and the version of the best model that included transfers from cellulosic and lignin pools had a dAICc of 931 (Table 3; Appendix S4).

Hypothesis 3: inhibition of biotic decomposition by exposure to shortwave radiation

In addition to increasing mass loss via abiotic photodegradation, solar radiation also reduced biotic decomposition of all pools in the best model ($1 - r$; Table 3). Indeed, all models with a dAICc < 13 included this term (Appendix S4). On

average across all sites, this function reduced the biotic decomposition rate of all pools by 70–90%, depending on litterbag ash content (less inhibition with increasing ash content). On average, biotic decomposition in the best model accounted for 2.5–7.8% per year during early-stage decomposition and 0.5–1.5% per year during late-stage decomposition, depending on ash content. Although mass losses from the cellulose and lignin pools were larger in the photodegradation model than in the biotic-only model (due to photodegradation fluxes that were larger than concurrent reductions in biotic decomposition), mass loss from the labile pool in the photodegradation model was substantially slower than in the biotic-only model due to the inhibition of biotic decomposition (Fig. 2). In the biotic-only model, the labile pool reached <1% of initial mass remaining by year 5, but in the best photodegradation model, 2% still remained at year 10 (on average).

Reducing biotic decomposition of labile carbon also provided a mechanism for a pattern found in the data: Compared to areas where biotic decomposition dominates, litter N content had a small or negligible impact on initial decomposition rates at these sites (Fig. 4). Litter types with dramatically different initial N decomposed at very similar rates during early-stage decomposition, a pattern captured by the best photodegradation model (Fig. 4a). This is in contrast to the biotic-only model predictions, where initial N content had a much larger impact on early-stage decomposition (Fig. 4b). Furthermore, there were no significant relationships between mass remaining and initial N at any time point (data not shown).

Hypothesis 4: reduction in photodegradation effects by soil infiltration

The best model contained a term that allowed soil infiltration to reduce photodegradation and reduce the inhibition of microbial decomposition by solar radiation (characterized as percent ash/ 100; Table 3, Model 42). For the slow (lignin) pool, ash content decreased annual mass loss due to photodegradation by 0.02% at low ash contents to 0.35% at high ash contents (on average across sites). For the slow cellulosic pool, ash content reduced annual photodegradation mass loss by a minimum of 0.09% at low ash and high initial lignin contents and by a maximum of 3.1%
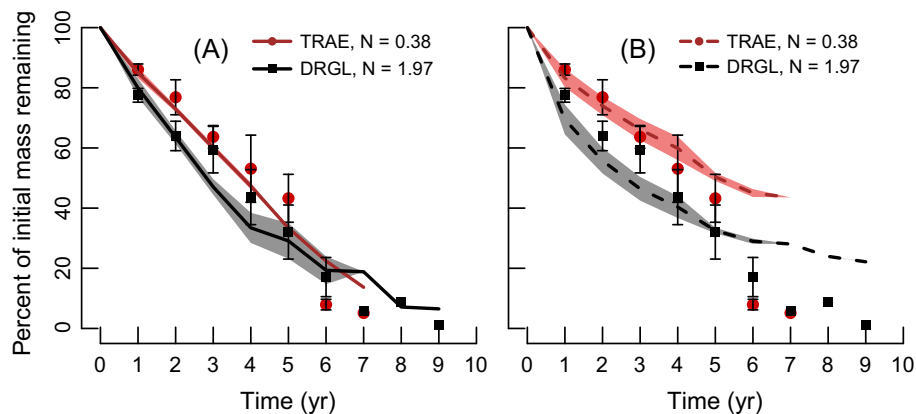
Fig. 4. Percent mass remaining over time averaged across sites for two litter types (*Triticum aestivum*, TRAE, and *Drypetes glauca*, DRGL) of different *N* contents (Table 2) with predictions from the (a) best photodegradation and (b) biotic-only models. Shaded areas and error bars are ±1 SE of averaged model predictions and observed data.

at high ash and low initial lignin contents. During early- and late-stage decomposition, shading by soil increased biotic decomposition by 5.3% and 1% per year, respectively.

DISCUSSION

Using a mass loss model that attempts to account for photodegradation in arid systems dramatically improved predictions of litter mass and *N* remaining, particularly over long timescales (>4 yr). This result is consistent with the work of Day et al. (2015), who found that the impact of photodegradation on mass loss increased with exposure to solar radiation (although over much shorter timescales). On average, the biotic-only and photodegradation models both over- and underestimated mass loss in years 1–4 by 5% or less, but failing to account for mass loss due to photodegradation—despite concurrent reductions in biotic decomposition—underestimated mass loss by 26% by year 10. In comparison, the best photodegradation model only under-predicted mass loss by 6% in year 10. Our results are consistent with a recent meta-analysis by King et al. (2012) that found mass loss in litter exposed to ambient solar radiation was 23% faster than in litter exposed to reduced solar radiation. Thus, models that do not account for photodegradation in arid systems may be dramatically under-predicting *C* loss, especially over longer time periods.

Furthermore, our results suggest that photodegradation alters litter *C* pool dynamics from those found in humid environments dominated by biotic decomposition by increasing mass loss from recalcitrant *C* pools. In the best model, the sources of mass loss due to photodegradation were both cellulosic and lignin *C* pools, although the majority of the mass lost in our model came from the cellulosic pool (Hypothesis 1). Of the total mass lost due to photodegradation each year, only 10–20% was from the lignin pool. The remaining 80–90% came from the cellulosic pool. Our results are consistent with research that has found photodegradation to increase mass loss from lignin (Day et al. 2007, Henry 2008, Austin and Ballaré 2010, Austin et al. 2016) and from cellulose (Lin and King 2014) and/or hemicellulose (Rozema et al. 1997, Brandt et al. 2010, King et al. 2012, Lin and King 2014, Lin et al. 2015*a*). However, our findings contrast with studies that have *not* found photodegradation to increase lignin mass loss (Gehrke et al. 1995, Brandt et al. 2007, 2010, King et al. 2012, Lin and King 2014, Baker and Allison 2015). Yet, our results indicate that rates of lignin photodegradation are relatively low (1.1–1.5% per year). Such low rates may not be detectable over the relatively short study periods (e.g., <1 year) of most photodegradation research. Thus, future studies may wish to focus on losses from these pools over the long term (>4–5 yr).

Based on previous short-term experiments (e.g., Austin and Ballaré 2010), we expected that higher litter lignin content would increase mass loss, not only through direct but also through indirect photolysis. Surprisingly, we found essentially no

evidence to suggest that lignin increased photodegradation of cellulosic material. In fact, mass loss decreased with increasing lignin content at most time points, and the best photodegradation model included a term that reduced photodegradation as a function of initial lignin content. On average, increasing initial lignin content reduced photodegradation from the cellulosic pool by half (from 14% to 7% per year; averaged across ash contents). Thus, our results are not supportive of lignin-induced increases in mass loss from cellulosic carbon pools (i.e., via indirect photolysis) and even suggest a lignin protection of cellulose from photodegradation. One explanation for our contrasting results may be the long duration of the LIDET study relative to the short-term nature of most photodegradation studies. Another potential explanation may be the different lignin assays used across studies. Here, we used the acid-non-hydrolyzable fraction as lignin. Other lignin assays, like the acetyl bromide method, may measure different compounds as lignin and may provide data to support the argument that lignin is vulnerable to UV radiation (Henry 2008). Still, the reasons for these contrasting results are not clear and suggest the need for continuing mechanistic experiments and combining long-term field experiments with more detailed examination of C pool dynamics over time.

The mass loss dynamics of C fractions in the photodegradation model were also different from those in the biotic-only model. Photodegradation increased mass loss from the cellulosic C pool *abiotically* while simultaneously suppressing *biotic* decomposition of the labile pool. The combination of these factors resulted in the "fast" or labile pool losing mass relatively slowly, while the slow cellulosic pool lost mass relatively quickly. This pattern directly contrasts predictions from biotic decomposition models, where labile pools (by definition) lose mass very quickly, usually disappearing by years 4–5. Lin et al. (2015*a*) found evidence of such atypical C dynamics in a field study: Exposure to UV caused declines in hemicellulose but increases in cell solubles (labile C).

In contrast to our second hypothesis, our model did not directly support facilitation of biotic decomposition via the incorporation of photodegraded lignin and cellulosic carbon into the labile C pool. Yet, recent work has found that exposing litter to solar radiation enhances biotic decomposition: Respiration or leaching increases during subsequent precipitation events in exposed relative to unexposed litter (Gallo et al. 2006, Feng et al. 2011, Foereid et al. 2011, Ma et al. 2012, Lin and King 2014, Baker and Allison 2015, Austin et al. 2016), and exposure to light has, in one case, been found to enhance the enzymatic breakdown of plant C compounds (Cannella et al. 2016). However, these studies have been, in the short term, focused on within-year time steps. It may be that these dynamics—the production of labile C from cellulosic or lignin C—cannot be captured using the yearlong time steps of the LIDET data; photodegraded products may be produced and lost from litterbags via biotic decomposition and/or leaching within a yearly time step (e.g., during dry and wet seasons).

In addition to enhancing litter mass loss, solar radiation can have direct negative impacts on microbial decomposition (Hypothesis 3; e.g., Johanson et al. 1995, Johnson 2003, Smith et al. 2010). Our results suggest that the exposure of litter to solar radiation reduces decomposition rates via negative impacts on soil decomposer populations (Hypothesis 3). The LIDET data and model results also suggest that litter N availability plays a much smaller role in dryland vs. humid systems, as N content had little impact on early mass loss rates. This limited role of N in early decomposition may be due to the reduced role of biotic decomposition that results from exposure to solar radiation. However, as mentioned above, the smallest time step in these data was approximately 1 year. It is possible that litter N plays a larger role at shorter timescales, for example, during wet periods when microbes are very active.

As hypothesized, we found that soil infiltration reduced both photodegradation and UV-induced inhibition of biotic decomposition (as represented by litter sample ash content; Hypothesis 4; Throop and Archer 2007). In the best model, increasing ash content reduced photodegradation by between 7% and 14% (depending on initial lignin content). Because the LIDET experiment was not specifically designed to test the effects of soil infiltration or soil shading on photodegradation, other studies may be able to reveal more significant soil shading impacts on biotic decomposers and abiotic decomposition.

Mixing may have other impacts that promote decomposition (e.g., physical abrasion and buffering from heat and aridity; Hewins et al. 2013, Lee et al. 2014), but litterbag studies, such as LIDET, are not well suited to investigate these impacts. Nevertheless, our results suggest that soil shading protects both litter and decomposers from the impacts of exposure to solar radiation, in agreement with recent work on the impacts of soil–litter mixing (Throop and Archer 2009, Barnes et al. 2012, 2015).

CONCLUSIONS

Overall, we found that incorporating photodegradation into our decomposition model increased the accuracy of long-term litter mass loss predictions in dryland systems, especially after four years. Our results also indicate that photodegradation may be a substantial mass loss vector: Photodegradation increased mass loss by 6–15% per year compared to biotic decomposition rates that ranged from 3% to 20% per year. Because much remains to be discovered about the mechanisms driving the impacts of litter exposure to solar radiation, the best model is not a comprehensively mechanistic representation of photodegradation and other solar radiation impacts. Despite this, our results suggest that even our relatively simplistic representation is a substantial improvement over an approach that disregards these impacts; failing to account for photodegradation under-predicted long-term litter mass by 26%. Furthermore, photodegradation resulted in C fraction dynamics that were different from traditional biotic decomposition models, suggesting that photodegradation slows losses from labile pools and accelerates losses from cellulosic and lignin pools.

As the climate continues to change, dryland systems are projected to expand globally, perhaps occupying 50% or more of the total land surface by the end of the century (Feng and Fu 2013, Huang et al. 2016). In such a setting, photodegradation will likely play a large role in controlling global and regional C cycling. Additionally, drylands are expected to become drier (Stocker et al. 2013), suggesting that there may be a shift in the balance between biotic and abiotic processes toward abiotic processes. Failing to account for the myriad impacts of photodegradation—accelerated mass loss, altered C transformations, and impacts on biotic decomposition—in C cycling models will therefore produce growing inaccuracies in our representations of C cycling that may result in large underestimations of C losses from these dryland systems.

LITERATURE CITED

Aber, J. D., J. M. Melillo, and C. A. McClaugherty. 1990. Predicting long-term patterns of mass-loss, nitrogen dynamics, and soil organic-matter formation from initial fine litter chemistry in temperate forest ecosystems. Canadian Journal of Botany 68:2201–2208.

Adair, E. C., W. J. Parton, S. J. Del Grosso, W. L. Silver, M. E. Harmon, S. A. Hall, I. C. Burke, and S. C. Hart. 2008. Simple three-pool model accurately describes patterns of long-term litter decomposition in diverse climates. Global Change Biology 14:2636–2660.

Austin, A. T., and C. L. Ballaré. 2010. Dual role of lignin in plant litter decomposition in terrestrial ecosystems. Proceedings of the National Academy of Sciences of the United States of America 107:4618–4622.

Austin, A. T., M. S. Méndez, and C. L. Ballaré. 2016. Photodegradation alleviates the lignin bottleneck for carbon turnover in terrestrial ecosystems. Proceedings of the National Academy of Sciences of the United States of America 113:4392–4397.

Baker, N. R., and S. D. Allison. 2015. Ultraviolet photodegradation facilitates microbial litter decomposition in a Mediterranean climate. Ecology 96:1994–2003.

Barnes, P. W., H. L. Throop, S. R. Archer, D. D. Breshears, R. L. McCulley, and M. A. Tobler. 2015. Sunlight and soil–litter mixing: drivers of litter decomposition in drylands. Pages 273–302 *in* U. Lüttge and W. Beyschlag, editors. Progress in botany. Volume 76. Springer, New York, New York, USA.

Barnes, P., H. Throop, D. Hewins, M. Abbene, and S. Archer. 2012. Soil coverage reduces

photodegradation and promotes the development of soil-microbial films on dryland leaf litter. Ecosystems 15:311–321.

Berg, B., G. Ekbohm, and C. McClaugherty. 1984. Lignin and holocellulose relations during long-term decomposition of some forest litters: long-term decomposition in a Scots pine forest 4. Canadian Journal of Botany 62:2540–2550.

Berg, B., K. Hannus, T. Popoff, and O. Theander. 1982. Changes in organic-chemical components of needle litter during decomposition - long-term decomposition in a Scots pine forest 1. Canadian Journal of Botany 60:1310–1319.

Bolker, B., and R Development Core Team 2016. bbmle: tools for general maximum likelihood estimation. R package. Version 1.0.18. https://CRAN.R-project.org/package=bbmle

Brandt, L. A., C. Bohnet, and J. Y. King. 2009. Photochemically induced carbon dioxide production as a mechanism for carbon loss from plant litter in arid ecosystems. Journal of Geophysical Research: Biogeosciences 114:1–13.

Brandt, L. A., J. Y. King, S. E. Hobbie, D. G. Milchunas, and R. L. Sinsabaugh. 2010. The role of photodegradation in surface litter decomposition across a grassland ecosystem precipitation gradient. Ecosystems 13:765–781.

Brandt, L. A., J. Y. King, and D. G. Milchunas. 2007. Effects of ultraviolet radiation on litter decomposition depend on precipitation and litter chemistry in a shortgrass steppe ecosystem. Global Change Biology 13:2193–2205.

Burnham, K. P., and D. R. Anderson. 2002. Model selection and multimodel inference: a practical information-theoretic approach, Second edition. Springer-Verlag, New York, New York, USA.

Caldwell, M. M., L. O. Björn, J. F. Bornman, S. D. Flint, G. Kulandaivelu, A. H. Teramura, and M. Tevini. 1998. Effects of increased solar ultraviolet radiation on terrestrial ecosystems. Journal of Photochemistry and Photobiology B: Biology 46:40–52.

Cannella, D., K. B. Möllers, N. U. Frigaard, P. E. Jensen, M. J. Bjerrum, K. S. Johansen, and C. Felby. 2016. Light-driven oxidation of polysaccharides by photosynthetic pigments and a metalloenzyme. Nature Communications 7:11134.

Chen, M., W. J. Parton, E. C. Adair, S. Asao, M. D. Hartman, and W. Gao. 2016. Simulation of the effects of photodecay on long-term litter decay using DayCent. Ecosphere 7:e01631.

Chesson, A. 1997. Plant degradation by ruminants: parallels with litter decomposition in soils. Pages 47–66 in G. Cadisch and K. E. Giller, editors. Driven by nature: plant litter quality and decomposition. CAB International, Wallingford, UK.

Day, T. A., R. Guénon, and C. T. Ruhland. 2015. Photodegradation of plant litter in the Sonoran Desert varies by litter type and age. Soil Biology and Biochemistry 89:109–122.

Day, T., E. Zhang, and C. Ruhland. 2007. Exposure to solar UV-B radiation accelerates mass and lignin loss of Larrea tridentata litter in the Sonoran Desert. Plant Ecology 193:185–194.

Effland, M. J. 1977. Modified procedure to determine acid-insoluble lignin in wood and pulp. Tappi 60:143–144.

Feng, S., and Q. Fu. 2013. Expansion of global drylands under a warming climate. Atmospheric Chemistry and Physics 13:10081–10094.

Feng, X., K. M. Hills, A. J. Simpson, J. K. Whalen, and M. J. Simpson. 2011. The role of biodegradation and photo-oxidation in the transformation of terrigenous organic matter. Organic Geochemistry 42:262–274.

Fernández Zenoff, V., F. Siñeriz, and M. E. Farías. 2006. Diverse responses to UV-B radiation and repair mechanisms of bacteria isolated from high-altitude aquatic environments. Applied and Environmental Microbiology 72:7857–7863.

Foereid, B., M. J. Rivero, O. Primo, and I. Ortiz. 2011. Modelling photodegradation in the global carbon cycle. Soil Biology and Biochemistry 43:1383–1386.

Gallo, M. E., R. L. Sinsabaugh, and S. E. Cabaniss. 2006. The role of ultraviolet radiation in litter decomposition in arid ecosystems. Applied Soil Ecology 34:82–91.

Gehrke, C., U. Johanson, T. V. Callaghan, D. Chadwick, and C. H. Robinson. 1995. The impact of enhanced ultraviolet-B radiation on litter quality and decomposition processes in Vaccinium leaves from the sub-arctic. Oikos 72:213–222.

Gholz, H. L., D. A. Wedin, S. M. Smitherman, M. E. Harmon, and W. J. Parton. 2000. Long-term dynamics of pine and hardwood litter in contrasting environments: toward a global model of decomposition. Global Change Biology 6:751–765.

Harmon, M. E., W. L. Silver, I. C. Burke, B. Fasth, W. J. Parton, and LIDET. 2009. Long-term patterns of mass loss during the decomposition of leaf and fine root litter: an across site comparison. Global Change Biology 15:1320–1338.

Henry, H. A. L. 2008. Climate change and soil freezing dynamics: historical trends and projected changes. Climatic Change 87:421–434.

Hewins, D., S. Archer, G. Okin, R. McCulley, and H. Throop. 2013. Soil–litter mixing accelerates decomposition in a Chihuahuan Desert grassland. Ecosystems 16:183–195.

Huang, J., H. Yu, X. Guan, G. Wang, and R. Guo. 2016. Accelerated dryland expansion under climate change. Nature Climate Change 6:166–171.

Johanson, U., C. Gehrke, L. O. Björn, T. V. Callaghan, and M. Sonesson. 1995. The effects of enhanced UV-B radiation on a subarctic heath ecosystem. Ambio 24:106–111.

Johnson, D. 2003. Response of terrestrial microorganisms to ultraviolet-B radiation in ecosystems. Research in Microbiology 154:315–320.

Kielbassa, C., L. Roza, and B. Epe. 1997. Wavelength dependence of oxidative DNA damage induced by UV and visible light. Carcinogenesis 18:811–816.

King, J. Y., L. A. Brandt, and E. C. Adair. 2012. Shedding light on plant litter decomposition: advances, implications and new directions in understanding the role of photodegradation. Biogeochemistry 111:57–81.

Kurbanyan, K., K. L. Nguyen, P. To, E. V. Rivas, A. M. Lueras, C. Kosinski, M. Streryo, A. Gonzales, D. A. Mah, and E. D. Stemp. 2003. DNA-protein cross-linking via guanine oxidation: dependence upon protein and photosensitizer. Biochemistry 42: 10269–10281.

Lee, H., J. Fitzgerald, D. B. Hewins, R. L. McCulley, S. R. Archer, T. Rahn, and H. L. Throop. 2014. Soil moisture and soil-litter mixing effects on surface litter decomposition: a controlled environment assessment. Soil Biology and Biochemistry 72:123–132.

Lin, Y., and J. Y. King. 2014. Effects of UV exposure and litter position on decomposition in a California grassland. Ecosystems 17:158–168.

Lin, Y., J. Y. King, S. Karlen, and J. Ralph. 2015a. Using 2D NMR spectroscopy to assess effects of UV radiation on cell wall chemistry during litter decomposition. Biogeochemistry 125:427–436.

Lin, Y., R. D. Scarlett, and J. Y. King. 2015b. Effects of UV photodegradation on subsequent microbial decomposition of *Bromus diandrus* litter. Plant and Soil 395:263–271.

Lloyd, J., and J. A. Taylor. 1994. On the temperature-dependence of soil respiration. Functional Ecology 8:315–323.

Long-term Intersite Decomposition Experiment Team (LIDET). 1995. Meeting the challenges of long term, broad scale ecological experiments. Publication number nineteen edition. U.S. LTER Network Office, Seattle, Washington, USA.

Ma, S., D. D. Baldocchi, J. A. Hatala, M. Detto, and J. Curiel Yuste. 2012. Are rain-induced ecosystem respiration pulses enhanced by legacies of antecedent photodegradation in semi-arid environments? Agricultural and Forest Meteorology 154–155:203–213.

McClaugherty, C., and B. Berg. 1987. Cellulose, lignin and nitrogen concentrations as rate regulating factors in late stages of forest litter decomposition. Pedobiologia 30:101–112.

McClaugherty, C. A., J. Pastor, J. D. Aber, and J. M. Melillo. 1985. Forest litter decomposition in relation to soil nitrogen dynamics and litter quality. Ecology 66:266–275.

Mitchell, D. L., and D. Karentz. 1993. The induction and repair of DNA photodamage in the environment. Pages 345–377 in A. R. Young, editor. Environmental UV photobiology. Plenum Press, New York, New York, USA.

North American Regional Reanalysis (NCEP). 2004. A long-term, consistent, high-resolution climate dataset for the North American domain, as a major improvement upon the earlier global reanalysis datasets in both resolution and accuracy. NOAA/OAR/ESRL PSD, Boulder, Colorado, USA. http://www.esrl.noaa.gov/psd/

Obst, J. R., and T. K. Kirk. 1988. Isolation of lignin. Pages 3–12 in W. A. Wood and S. T. Kellogg, editors. Methods in enzymology/biomass. Academic Press, New York, New York, USA.

Pancotto, V. A., O. E. Sala, T. M. Robson, M. M. Caldwell, and A. L. Scopel. 2005. Direct and indirect effects of solar ultraviolet-B radiation on long-term decomposition. Global Change Biology 11:1982–1989.

Parton, W., et al. 2007. Global-scale similarities in nitrogen release patterns during long-term decomposition. Science 315:361–364.

R Core Team. 2016. R: a language and environment for statistical computing. R Foundation for Statistical Computing, Vienna, Austria.

Rozema, J., M. Tosserams, H. J. M. Nelissen, L. vanHeerwaarden, R. A. Broekman, and N. Flierman. 1997. Stratospheric ozone reduction and ecosystem processes: enhanced UV-B radiation affects chemical quality and decomposition of leaves of the dune grassland species *Calamagrostis epigeios*. Plant Ecology 128:284–294.

Ryan, M. G., J. M. Melillo, and A. Ricca. 1990. A comparison of methods for determining proximate carbon fractions of forest litter. Canadian Journal of Forest Research 20:166–171.

Schade, G. W., R.-M. Hofmann, and P. J. Crutzen. 1999. CO emissions from degrading plant matter. Tellus Series B 51:889–908.

Smith, W. K., W. Gao, H. Steltzer, M. D. Wallenstein, and R. Tree. 2010. Moisture availability influences the effect of ultraviolet-B radiation on leaf litter decomposition. Global Change Biology 16:484–495.

Stocker, T. F., et al. 2013. Technical summary. Pages 79–113 in T. F. Stocker, editor. Climate Change

2013: the Physical Science Basis. Contribution of Working Group I to the Fifth Assessment Report of the Intergovernmental Panel on Climate Change. Cambridge University Press, Cambridge, UK.

Throop, H. L., and S. R. Archer. 2007. Interrelationships among shrub encroachment, land management, and litter decomposition in a semidesert grassland. Ecological Applications 17:1809–1823.

Throop, H., and S. Archer. 2009. Resolving the dryland decomposition conundrum: some new perspectives on potential drivers. Pages 171–194 *in* U. Lüttge,

W. Beyschlag, B. Büdel, and D. Francis, editors. Progress in botany. Springer, Berlin, Germany.

Uselman, S. M., K. A. Snyder, R. R. Blank, and T. J. Jones. 2011. UVB exposure does not accelerate rates of litter decomposition in a semi-arid riparian ecosystem. Soil Biology and Biochemistry 43:1254–1265.

Wang, J., L. Liu, X. Wang, and Y. Chen. 2015. The interaction between abiotic photodegradation and microbial decomposition under ultraviolet radiation. Global Change Biology 21:2095–2104.

Supporting Information